

WATER ABUNDANCE IN MOLECULAR CLOUD CORES

R. L. SNELL¹, J. E. HOWE¹, M. L. N. ASHBY², E. A. BERGIN², G. CHIN³, N. R. ERICKSON¹, P. F. GOLDSMITH⁴, M. HARWIT⁵, S. C. KLEINER², D. G. KOCH⁶, D. A. NEUFELD⁷, B. M. PATTEN², R. PLUME², R. SCHIEDER⁸, J. R. STAUFFER², V. TOLLS², Z. WANG², G. WINNEWISSER⁸, Y. F. ZHANG²,
 AND G. J. MELNICK²

Received 2000 March 27; accepted 2000 June 21; published 2000 August 16

ABSTRACT

We present *Submillimeter Wave Astronomy Satellite* (SWAS) observations of the $1_{10} \rightarrow 1_{01}$ transition of ortho- H_2O at 557 GHz toward 12 molecular cloud cores. The water emission was detected in NGC 7538, ρ Oph A, NGC 2024, CRL 2591, W3, W3(OH), Mon R2, and W33, and was not detected in TMC-1, L134N, and B335. We also present a small map of the H_2O emission in S140. Observations of the H_2^{18}O line were obtained toward S140 and NGC 7538, but no emission was detected. The abundance of ortho- H_2O relative to H_2 in the giant molecular cloud cores was found to vary between 6×10^{-10} and 1×10^{-8} . Five of the cloud cores in our sample have previous H_2O detections; however, in all cases the emission is thought to arise from hot cores with small angular extents. The H_2O abundance estimated for the hot core gas is at least 100 times larger than in the gas probed by SWAS. The most stringent upper limit on the ortho- H_2O abundance in dark clouds is provided in TMC-1, where the 3σ upper limit on the ortho- H_2O fractional abundance is 7×10^{-8} .

Subject headings: ISM: abundances — ISM: clouds — ISM: molecules — radio lines: ISM

1. INTRODUCTION

The *Submillimeter Wave Astronomy Satellite* (SWAS) has detected spatially extended H_2O emission associated with the quiescent dense molecular gas in Orion and M17 (Snell et al. 2000a,b). Based on these observations the relative abundance of ortho- H_2O was found to be surprisingly small, ranging from only 1×10^{-9} to 8×10^{-8} . We present here SWAS observations of the ortho- H_2O transition at 557 GHz in the three dark cloud cores TMC-1, L134N and B335 and in the nine giant molecular cloud cores W3, W3(OH), Mon R2, ρ Oph A, W33, CRL 2591, S140, and NGC 7538.

Five of the cloud cores in our survey have had previously reported water detections. NGC 7538, S140, W3, and CRL 2591 were detected by the *Infrared Space Observatory* in the ro-vibrational lines of H_2O from the ν_2 bending mode at $6 \mu\text{m}$ in absorption against the dust continuum (van Dishoeck & Helmich 1996; Helmich et al. 1996; van Dishoeck 1998). Water emission has also been detected in NGC 7538, W3, and W3(OH) from the $3_{13} \rightarrow 2_{20}$ transition of H_2O at 183 GHz (Cernicharo et al. 1990) and the $3_{13} \rightarrow 2_{20}$ transition of H_2^{18}O at 203 GHz (Gensheimer, Mauersberger, & Wilson 1996). The 183 GHz and 203 GHz lines arise from transitions with relatively high energies ($E_u/k \gtrsim 200$ K) and thus are likely produced in relatively warm gas. The $6 \mu\text{m}$ absorption features can arise from a range of gas temperatures, however the absorption seen in these sources is thought to be dominated by relatively warm gas. The relative abundance of H_2O in the warm gas has been estimated to be 1×10^{-6} to 1×10^{-4} . SWAS, on the other hand, can observe the lowest energy rotational transi-

tion of ortho- H_2O permitting detection of H_2O emission from the more extended, cold core gas. We estimate the abundance of ortho-water in the relatively cold ($T < 50$ K) core gas and compare the abundance results with those for the warm gas and those for Orion and M17.

2. OBSERVATIONS AND RESULTS

The observations of H_2O and H_2^{18}O reported here were obtained by SWAS during the period 1998 December to 2000 January. The data were acquired by nodding the satellite alternatively between the cloud core and a reference position free of molecular emission. Details concerning data acquisition, calibration, and reduction with SWAS are presented in Melnick et al. (2000). Observations of the $1_{10} \rightarrow 1_{01}$ transition of H_2O at a frequency of 556.936 GHz were obtained toward the positions given in Table 1. Total integration times for these observations range from 17 hr for W3(OH) to 127 hr for L134N.

In addition, we obtained a small 10-point map of the S140 cloud core with integration times per position of between 18 and 36 hr. The center positions of S140 and NGC 7538 were also observed in H_2^{18}O at a frequency of 547.676 GHz for 189 and 36 hr respectively. The SWAS beam is elliptical, and at the frequency of the water transitions has angular dimensions of $3'.3 \times 4'.5$. The data shown in this paper are in antenna temperature units and are not corrected for the measured SWAS main beam efficiency of 0.90. We also used the Five College Radio Astronomy Observatory (FCRAO) 14 m telescope to map the $J = 1 \rightarrow 0$ transition of C^{18}O in an approximately $6' \times 6'$ region in each core to provide an estimate of the gas column density

¹ Department of Astronomy, University of Massachusetts, Amherst, MA 01003

² Harvard-Smithsonian Center for Astrophysics, 60 Garden Street, Cambridge, MA 02138

³ NASA Goddard Spaceflight Center, Greenbelt, MD 20771

⁴ National Astronomy and Ionosphere Center, Department of Astronomy, Cornell University, Space Sciences Building, Ithaca, NY 14853-6801

⁵ 511 H Street SW, Washington, DC 20024-2725; also Cornell University

⁶ NASA Ames Research Center, Moffett Field, CA 94035

⁷ Department of Physics and Astronomy, Johns Hopkins University, 3400 North Charles Street, Baltimore, MD 21218

⁸ I. Physikalisches Institut, Universität zu Köln, Zùlpicher Strasse 77, D-50937 Köln, Germany

TABLE 1
WATER LINE PARAMETERS AND ABUNDANCE DETERMINATION

Source	R.A. (J2000)	Decl. (J2000)	$\int T_A^* dv$ (K km s ⁻¹)	$\sigma(\int T_A^* dv)$ (K km s ⁻¹)	Temperature (K)	log n (cm ⁻³)	$x(\text{o-H}_2\text{O})$
W3	02 25 29.9	+62 05 54	2.93	0.13	45	6.0	2×10^{-9}
W3(OH)	02 27 02.8	+61 52 21	2.93	0.13	30	6.3	2×10^{-9}
TMC-1	04 41 20.4	+25 47 52	...	0.02	10	4.8	$< 7 \times 10^{-8}$
NGC 2024	05 41 44.5	-01 55 35	0.83	0.06	35	6.0	6×10^{-10}
Mon R2	06 07 40.2	-06 23 28	0.90	0.07	40	5.6	2×10^{-9}
L134N	15 54 06.5	-02 52 19	...	0.02	10	4.3	$< 3 \times 10^{-7}$
ρ Oph	16 26 19.3	-24 24 02	0.81	0.05	30	5.5	3×10^{-9}
W33	18 14 15.1	-17 55 25	0.46	0.08	23	5.7	1×10^{-9}
B335	19 36 58.7	+07 33 47	...	0.02	10	4.3	$< 1 \times 10^{-6}$
CRL 2591	20 29 25.9	+40 11 19	0.34	0.04	38	5.1	6×10^{-9}
S140	22 19 17.1	+62 18 46	1.71	0.08	30	5.8	8×10^{-9}
NGC 7538	23 13 47.6	+61 26 54	3.09	0.10	25	6.0	1×10^{-8}

Note. — Units of right ascension are hours, minutes, and seconds, and units of declination are degrees, arcminutes, and arcseconds.

for use in our analysis of the H₂O data.

H₂O emission was detected in all nine giant molecular cloud cores. However despite deep integrations, we were unable to detect H₂O emission in any of the three dark cloud cores. The H₂O spectra obtained for six of the cloud cores are shown in Figure 1. Spectra for five of the remaining six cores are shown in Ashby et al. (2000a). The spectrum of B335, where no H₂O emission was detected, is not shown. The H₂O line profiles for the giant molecular cloud cores show a wide variety of shapes, ranging from relatively narrow single-peaked lines to broad, strongly self-absorbed lines. We have marked in Figure 1 the line center velocity of the ¹³CO $J = 5 \rightarrow 4$ emission (J. Howe et al. 2000, in preparation) observed simultaneously with SWAS. In W3, Mon R2, and W33 it is obvious that the H₂O line is self-absorbed, since the peak of the ¹³CO emission corresponds to a minimum in the H₂O emission. CRL 2591 is probably also self-absorbed, although in this case the situation is somewhat more ambiguous. More discussion about the H₂O line profiles can be found in Ashby et al. (2000a). The spectra for ρ Oph A and NGC 7538 presented in Ashby et al. (2000a) show obvious broad wings, suggesting that some of the H₂O emission probably arises in associated molecular outflows.

A small map of the H₂O emission in S140 is shown in Figure 2. The emission toward the center of the core reveals a rela-

tively narrow ($\Delta V_{\text{FWHM}} = 5.7 \text{ km s}^{-1}$), single-peaked line. H₂O emission was also detected at positions 3'² to the north and south of center, however no emission was found east or west of center. The off-center spectra in general have rms noise of 0.02 K, about 2 times larger than the center position. During these observations the long axis of the SWAS beam was oriented approximately north-south, thus explaining the stronger emission detected in these directions.

We failed to detect H₂¹⁸O emission in either S140 or NGC 7538. The rms noise achieved in the NGC 7538 observation of 0.03 K was not adequate to place a very useful limit on the H₂O/H₂¹⁸O ratio. In S140, however, the H₂¹⁸O spectrum had an rms noise of only 0.01 K. In S140 we used the line width and line center velocity derived from a Gaussian fit to the H₂O line (see Fig. 2) to constrain a Gaussian fit to the H₂¹⁸O spectra. From this constrained fit we derived a 1σ upper limit to the integrated intensity of 0.022 K km s⁻¹ leading to a 1σ lower limit on the intensity ratio of H₂O/H₂¹⁸O of 70.

3. DETERMINATION OF THE WATER ABUNDANCE

We have analyzed the H₂O observations of the twelve cores

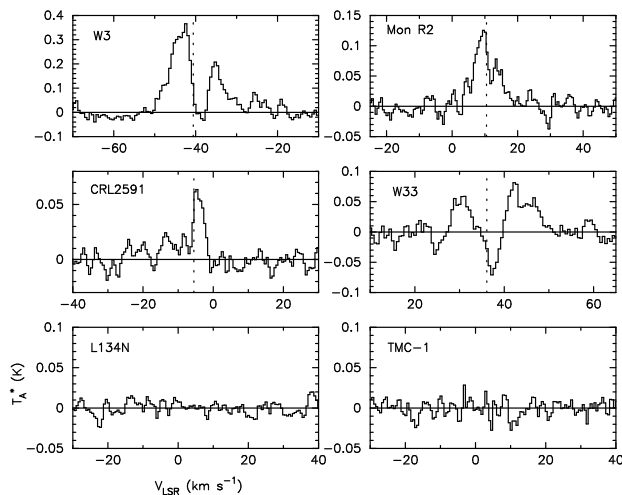


FIG. 1.— Spectra of the $1_{10} \rightarrow 1_{01}$ transition of ortho-H₂O from six cloud cores. The line center velocity of the ¹³CO $J = 5 \rightarrow 4$ transition observed simultaneously with SWAS is indicated for W3, Mon R2, CRL 2591, and W33 by a dotted line. The coordinates of each core are given in Table 1.

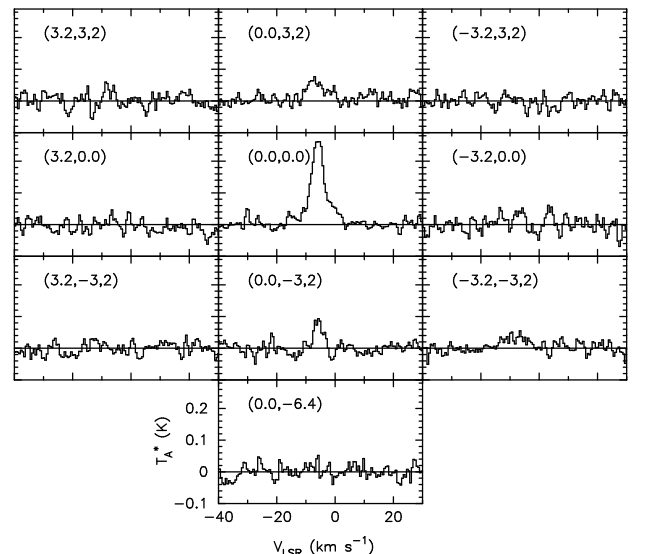


FIG. 2.— 10-position map of the $1_{10} \rightarrow 1_{01}$ transition of ortho-H₂O obtained with SWAS toward S140. The spectra were obtained on a regular grid spaced by 3'² and are shown in their correct relative positions on the sky. Offsets in arcminutes relative to the position of S140 given in Table 1 are indicated for each spectrum.

in the same manner as reported for Orion and M17 (Snell et al. 2000a, 2000b). Before reviewing this procedure, it is worth noting that the critical density for the 557 GHz transition of H_2O observed by *SWAS* is of order 10^8 cm^{-3} , much higher than the average density of gas in these cores. Therefore the probability of collisional deexcitation of this transition is very small, and photons produced by collisional excitations will all escape the cloud core, although they may be repeatedly absorbed and reemitted. A linear relation thus exists between the observed line integrated intensity and the product of the density and the ortho- H_2O column density, independent of the optical depth of this transition (Linke et al. 1977; Snell et al. 2000a). The emission in this case is effectively optically thin. Although we did not use this analytical expression to derive abundances, it provides insight into the dependence of the water abundance on the physical properties of the cloud.

We estimate the relative ortho- H_2O abundance using a simple model of the temperature, density, column density, and velocity dispersion for the gas in each core. The gas column density distribution was determined from the C^{18}O maps, sampled at $44''$ intervals, assuming LTE and a $\text{C}^{18}\text{O}/\text{H}_2$ abundance ratio of 1.7×10^{-7} . The *SWAS* beam filling factor is effectively the convolution of the column density distribution with the *SWAS* beam pattern. The velocity dispersion of the gas along each line of sight was determined from the C^{18}O line width. Another important parameter in our modeling is the gas density. For five sources (W3, W3(OH), ρ Oph, W33, and Mon R2) we have strip maps of the $\text{CS } J = 2 \rightarrow 1$ emission obtained at FCRAO and the $J = 5 \rightarrow 4$ and $J = 7 \rightarrow 6$ transitions obtained at KOSMA. Most of this data is unpublished, although the results for the core centers can be found in Trojan (2000). The CS emission was found to be centrally peaked in these cores with detectable emission extending at least several arcminutes from the center. Modeling of these data suggests that even though the column density decreases rapidly away from the core center, the density remains relatively constant. We used the published density results for L134N (Dickens et al. 2000), TMC-1 (Pratap et al. 1997), S140 (Snell et al. 1984; Zhou et al. 1994), NGC 2024 (Snell et al. 1984; Schulz et al. 1991), B335 (Zhou et al. 1993), NGC 7538 (Plume et al. 1997) and CRL 2591 (Carr et al. 1995; van Dishoeck et al. 1999) in our modeling. For L134N, TMC-1, S140, and NGC 2024 these authors have found that the density is relatively constant across the core. Thus for many of the cores the high column density gas, which dominates the *SWAS* emission, can be roughly characterized by a single density. We therefore assumed a constant density and temperature for the cores, and the values used are summarized in Table 1. Although a single density cannot apply to all of the gas within the *SWAS* beam, we believe that the use of this approximation should not lead to serious errors in our abundance determinations.

The collisional excitation of H_2O was computed using both the para- and ortho- H_2 collision rates with ortho- H_2O (Phillips, Maluendes, & Green 1996), and assuming a ratio of ortho- to para- H_2 given by LTE at the temperatures given in Table 1. We did not include dust in our model, however the calculations of Ashby et al. (2000b) for S140 and ρ Oph A indicate that the exclusion of the dust continuum emission will have only a minor impact on the determination of the water abundance. We do note that in W33, the line is clearly absorbing the dust continuum, and therefore some of the dust continuum photons are converted into line photons. For our analysis we have used the total integrated intensity including the negative contribution in

the absorption feature, and thus, the integrated line intensity should be representative of the total number of line photons.

We proceed in our analysis by guessing a relative ortho- H_2O abundance for the core, then computing the emission distribution, and finally convolving that distribution with the *SWAS* beam. The abundance of H_2O is varied until the modeled integrated intensity agrees with observations. We assume a constant H_2O abundance across each source. For positions with no detections, we used the 3σ upper limit on the integrated intensity to establish a 3σ upper limit on the H_2O abundance. The abundances and/or limits found for each core are given in Table 1. For S140 and ρ Oph A our results agree well with the abundances derived by Ashby et al. (2000b) using a more detailed 3-dimensional model of the density and temperature profile within these sources. The uncertainty in our derived abundances is dominated by the uncertainties in the physical conditions, chiefly density. The accuracy of density determinations is of order a factor of three, thus leading to abundance uncertainties of the same magnitude. However, due to our use of a single density to characterize these cores, the gas density at the periphery of the cloud cores may be overestimated. This does not have a big impact on the abundance determination because the column density is low in these regions and does not contribute substantially to the H_2O emission detected by *SWAS*. Nevertheless, the use of a single density slightly biases our abundance determinations toward lower values.

In the giant molecular cloud cores the abundance of ortho- H_2O relative to H_2 varies from 6×10^{-10} to 1×10^{-8} . The highest H_2O abundances are derived for NGC 7538 and S140. The high H_2O abundance found for NGC 7538 is in part a consequence of including emission arising from the molecular outflows, thus resulting in an overestimate of the core abundance. However, in S140, the line profile is relatively narrow and it is unlikely that the core emission is substantially contaminated by outflow emission.

We have also analyzed the mapping data for S140 using the same model as used for the center position. The detected H_2O emission at positions $3/2$ north and $3/2$ south of center is consistent with the predictions based on our cloud model using the abundance of H_2O found for the core center. The cloud core is extended to the north-east, and the absence of H_2O emission toward the positions east and north-east of the core center requires that either the abundance of ortho- H_2O or the gas density be about 2 to 4 times smaller than toward the core center. The absence of extended emission in the higher rotational transitions of CS (Snell et al. 1984), suggests that the lack of H_2O emission is most likely explained by a lower density and not a lower abundance. The non-detections of H_2O emission in the remaining positions is entirely consistent with our cloud model and the H_2O abundance reported in Table 1.

Although we believe that for most of the gas the H_2O emission is effectively thin, it is possible that there are very small dense knots of gas that are not. In addition, a relatively thin layer of gas in an extended envelope surrounding the core could have sufficient H_2O optical depth to scatter the line photons that arise from the core (Snell et al. 2000a). The H_2^{18}O line should be less sensitive to these problems since it is optically thin, and therefore a more reliable estimator of the H_2O abundance. We have used the H_2^{18}O observations toward the S140 core to establish an upper limit to the fractional abundance of ortho- H_2O . Using the same physical model described above, we derive a 3σ upper limit to the ortho- H_2^{18}O abundance of 3×10^{-10} . As-

suming a ratio of $\text{H}_2\text{O}/\text{H}_2^{18}\text{O}$ of 500, this corresponds to a 3σ upper limit of 1×10^{-7} for the abundance of ortho- H_2O relative to H_2 . Comparing this result to our estimate of the H_2O abundance obtained from the more common isotopic species, it is not surprising that we were unable to detect H_2^{18}O in this core.

We failed to detect H_2O emission from the three dark cloud cores observed by *SWAS*. Although we achieved similar signal-to-noise ratio in all three cores, the higher density and column density in TMC-1 permit establishing a more stringent limit on the ortho- H_2O abundance. In TMC-1, we find a 3σ upper limit on the fractional abundance of ortho- H_2O of 7×10^{-8} . However, even in TMC-1 the water abundance limit is nearly two orders of magnitude larger than the typical giant molecular cloud core. The lower density and temperature in dark cloud cores make detection of H_2O very difficult.

4. DISCUSSION AND SUMMARY

SWAS has detected thermal water emission from nine giant molecular cloud cores which permit us to make the first estimate of the water abundance in the cold, dense core gas. The abundance of ortho- H_2O relative to H_2 in these cloud cores varies from 6×10^{-10} to 1×10^{-8} . The relative ortho- H_2O abundance in the majority of these cores is of order 1×10^{-9} , similar to the abundances found for M17SW (Snell et al. 2000b). In S140 the relative abundance of ortho- H_2O is about ten times larger, closer to the average ortho- H_2O abundance of Orion (Snell et al. 2000a). In general the relative abundance of ortho- H_2O found in these cores is inconsistent with chemical equilibrium models of well-shielded regions of clouds (Bergin, Melnick, & Neufeld 1998), even considering the most extreme uncertainties that might arise in our modeling procedure. Possible explanations for this discrepancy are discussed in Bergin et al. (2000).

Water has been previously detected from the hot gas in W3 IRS 5, W3(OH), CRL 2591, S140, and NGC 7538 IRS 1 via the 183 and 203 GHz emission lines and the ro-vibrational absorption lines at $6 \mu\text{m}$ (van Dishoeck & Helmich 1996; Helmich et al. 1996; Gensheimer et al. 1996; van Dishoeck 1998). It is worth noting that the *SWAS* observation of W3 is centered about midway between IRS 4 and IRS 5, less than $1'$ from IRS 5; and the *SWAS* observation of NGC 7538 is centered about $1'$ south of IRS 1. In both cases the regions probed via the $6 \mu\text{m}$, 183 GHz, and 203 GHz transitions are well within the *SWAS* beam. The water emission and absorption in these cores is thought to arise from hot cores surrounding young, massive stars with angular extents of only a few arcseconds and gas temperatures $\gtrsim 300$ K (van Dishoeck 1998; van Dishoeck et al. 1999). Abundance estimates for water in the hot cores range from 1×10^{-6} to 1×10^{-4} , several orders of magnitude greater than the abundance of water in the surrounding core gas. Even our limit on the H_2O abundance based on H_2^{18}O in S140 rules out the possibility that the large H_2O abundance found for the warm gas applies to the general cloud core. At temperatures exceeding ~ 200 – 400 K, found in shocks and hot cores, a series of neutral-neutral reactions rapidly converts nearly all of the gas phase oxygen into water (Charnley 1997; Bergin et al. 1998). Thus,

the substantial difference predicted by the gas-phase chemistry models for the water abundance in warm and cold gas is confirmed by our observations.

SWAS, with a large beam size and the ability to observe a low excitation line of water, is most sensitive to the water emission from the extended, colder dense gas. However, if the water abundance in the cold gas is extremely small, then the hot cores may still contribute to the emission seen by *SWAS*. If we assume that the brightness temperature of the 557 GHz emission from the hot core gas is 300 K (the same excitation temperature as implied by the absorption lines seen by *Infrared Space Observatory*) and that the core has an angular size of at most $2''$, then the contribution to the observed *SWAS* H_2O emission is negligible in most sources, except CRL 2591. Although van der Tak et al. (1999) suggest that the CRL 2591 hot core has an angular diameter much less than $1''$, the extremely weak emission detected in this source could have a significant hot-core contribution. Further information on the temperature and angular size of the hot core is needed to evaluate this possibility. If a significant fraction of the water emission detected by *SWAS* in CRL 2591 is attributed to the hot core, then the abundance of H_2O in the cold gas is even smaller than that quoted in Table 1.

Only upper limits to the ortho- H_2O abundance could be established for the dark cloud cores. If the abundance of water in these cores is as small as that found for the giant molecular cloud cores, it will be difficult to detect water emission in quiescent dark cloud cores. The most stringent limit on the ortho- H_2O abundance is set in TMC-1, and in this core the 3σ upper limit on the H_2O abundance is just marginally consistent with equilibrium gas-phase chemistry predictions (Bergin et al. 2000). B335 is the site of a well-studied class 0 protostar, while neither L134N nor TMC-1 are actively forming stars. Broad H_2O emission has been detected by *SWAS* toward two other class 0 protostellar cores, L1157 and NGC 1333 IRAS 4 (Neufeld et al. 2000). The H_2O emission in these sources clearly arises from the molecular outflows associated with class 0 sources. The relative abundance of ortho- H_2O in the outflow gas found by Neufeld et al. (2000) is of order 1×10^{-6} , considerably larger than the limit set in the two non-star forming cores, L134N and TMC-1. Neufeld et al. (2000) suggests that the enhanced abundance is due to shocks that convert a large fraction of the gas-phase oxygen into water. B335 also has an associated molecular outflow, with a outflow mass between that of L1157 and NGC 1333 IRAS 4 (Moriarty-Schieven & Snell 1989; Neufeld et al. 2000). The absence of H_2O emission in B335 is difficult to understand, unless either the density of the outflow gas is much lower than in L1157 or NGC 1333 IRAS 4, or the shock velocities are sufficiently small that H_2O formation by neutral-neutral reactions is inhibited.

This work was supported by NASA's *SWAS* contract NAS5-30702 and NSF grant AST97-25951 to the Five College Radio Astronomy Observatory. R. Schieder and G. Winnewisser would like to acknowledge the generous support provided by the DLR through grants 50 0090 090 and 50 0099 011.

REFERENCES

- Ashby, M. L. N., et al. 2000a, *ApJ*, 539, L115
 Ashby, M. L. N., et al. 2000b, *ApJ*, 539, L119
 Bergin, E. A., Melnick, G. J., & Neufeld, D. A. 1998, *ApJ*, 499, 777
 Bergin, E. A., et al. 2000, *ApJ*, 539, L129
 Carr, J. S., Evans, N. J., II, Lacy, J. H., & Zhou, S. 1995, *ApJ*, 450, 667
 Cernicharo, J., Thum, C., Hein, H., John, D., Garcia, P., & Mattiocco, F. 1990, *A&A*, 231, L15
 Charnley, S. B., 1997, *ApJ*, 481, 396

- Dickens, J. E., Irvine, W. M., Snell, R. L., Bergin, E. A., Schloerb, F. P., Pratap, P., & Miralles, M. P. 2000, *ApJ*, in press
- Gensheimer, P. D., Mauersberger, R., & Wilson, T. L. 1996, *A&A*, 314, 281
- Helmich, F. P., et al. 1996, *A&A*, 315, L173
- Linke, R. A., Goldsmith, P. F., Wannier, P. G., Wilson, R. W., & Penzias, A. A. 1977, *ApJ*, 214, 50
- Melnick G. J., et al. 2000, *ApJ*, 539, L77
- Moriarty-Schieven, G. H., & Snell, R. L. 1989, *ApJ*, 338, 952
- Neufeld, D. A., et al. 2000, *ApJ*, 539, L107
- Phillips, T. R., Maluendes, S., & Green, S. 1996, *ApJS*, 107, 467
- Plume, R., Jaffé, D. T., Evans, N. J., II, Martín-Pintado, J., & Gómez-González, J. 1997, *ApJ*, 476, 730
- Pratap, P., Dickens, J. E., Snell, R. L., Miralles, M. P., Bergin, E. A., Irvine, W. M., & Schloerb, F. P. 1997, *ApJ*, 486, 862
- Schulz, A., Güsten, R., Zylka, R., Serabyn, E. 1991, *A&A*, 246, 570
- Snell, R. L., Mundy, L. G., Goldsmith, P. F., Evans, N. J., II, & Erickson, N. R. 1984, *ApJ*, 276, 625
- Snell, R. L., et al. 2000a, *ApJ*, 539, L93
- Snell, R. L., et al. 2000b, *ApJ*, 539, L97
- Trojan, C. 2000, Ph.D. thesis, Universität zu Köln
- van der Tak, F. F. S., van Dishoeck, E. F., Evans, N. J., II, Bakker, E. J., & Blake, G. A. 1999, *ApJ*, 522, 991
- van Dishoeck, E. F. 1998, *Faraday Discuss.*, 109, 31
- van Dishoeck, E. F., & Helmich, F. P. 1996, *A&A*, 315, L177
- van Dishoeck, E. F., et al. 1999, in *The Universe as Seen by ISO*, ed. P. Cox, & M. F. Kessler, (ESA SP-427; Noordwijk: ESA/ESTEC), 437
- Zhou, S., Butner, H. M., Evans, N. J., II, Güsten, R., Kutner, M. L., & Mundy, L. G. 1994, *ApJ*, 428, 219
- Zhou, S., Evans, N. J., II, Kömpe, C., & Walmsley, C. M. 1993, *ApJ*, 404, 232